JACS
JOURNAL OF THE AMERICAN CHEMICAL SOCIETY
Article
pubs.acs.org/JACS

Entropic Contribution of Elongation Factor P to Proline Positioning at the Catalytic Center of the Ribosome

Lili K. Doerfel,[†,#] Ingo Wohlgemuth,[†,#] Vladimir Kubyshkin,[‡] Agata L. Starosta,[§,⊥] Daniel N. Wilson,[*,§,∥] Nediljko Budisa,[*,‡] and Marina V. Rodnina[*,†]

[†]Department of Physical Biochemistry, Max Planck Institute of Biophysical Chemistry, Am Fassberg 11, 37077 Goettingen, Germany
[‡]Institut für Chemie, Technische Universität Berlin, 10623 Berlin, Germany
[§]Gene Center and Department for Biochemistry, University of Munich, 81377 Munich, Germany
[∥]Center for integrated Protein Science Munich (CiPSM), University of Munich, 81377 Munich, Germany

Supporting Information

ABSTRACT: The peptide bond formation with the amino acid proline (Pro) on the ribosome is slow, resulting in translational stalling when several Pro have to be incorporated into the peptide. Stalling at poly-Pro motifs is alleviated by the elongation factor P (EF-P). Here we investigate why Pro is a poor substrate and how EF-P catalyzes the reaction. Linear free energy relationships of the reaction on the ribosome and in solution using 12 different Pro analogues suggest that the positioning of Pro-tRNA in the peptidyl transferase center is the major determinant for the slow reaction. With any Pro analogue tested, EF-P decreases the activation energy of the reaction by an almost uniform value of 2.5 kcal/mol. The main source of catalysis is the favorable entropy change brought about by EF-P. Thus, EF-P acts by entropic steering of Pro-tRNA toward a catalytically productive orientation in the peptidyl transferase center of the ribosome.

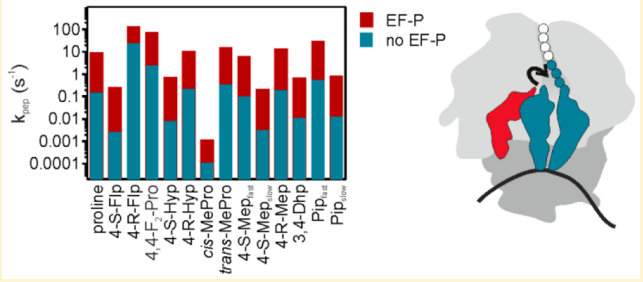

INTRODUCTION

The role of the ribosome is to translate genetic information encoded within mRNA into an amino acid sequence. Polymerization of amino acids on the ribosome occurs at the peptidyl transferase center and involves the accurate placement of the substrates to allow nucleophilic attack of the α-amino group of the aminoacyl-tRNA in the A site onto the carbonyl-carbon of the peptidyl-tRNA in the P site.[1] While the rate of this polymerization may vary for each amino acid,[2] previous studies have indicated that the proline (Pro) is not only a poor A-site acceptor of peptidyl moiety during peptide bond formation[3,4] but also acts as a poor donor when present in the P site.[2,5,6] Indeed, there is a wealth of evidence illustrating that the presence of proline within the polypeptide chain can have a dramatic influence on the efficiency of translation. For example, proline is present in many leader peptide sequences that are known to induce translational stalling such as the bacterial SecM and TnaC as well as the human cytomegalovirus (CMV) uORF2 of gp24.[7] Proline-containing motifs have been identified that promote ribosome stalling during translation elongation and termination, leading to subsequent tmRNA-mediated tagging.[8−10] Similarly, ribosome profiling identified the proline-containing tripeptide motifs as sites of ribosome accumulation.[11,12] Recent studies revealed that ribosome stalling is most dramatic when stretches of three or more consecutive proline residues occur in proteins.[5,10,13] In this situation, the ribosome stalling occurs because of slow peptide bond formation between the peptidyl-Pro-Pro-tRNA located in the P site and with the Pro-tRNA located in the A site (PP/P).[5,10] Interestingly, ribosome stalling at PP and PPP motifs is influenced by the context of the nascent polypeptide chain, in particular, the amino acids directly flanking the proline residues.[12,14−17]

Ribosome stalling at polyproline motifs is relieved by the translation elongation factor P (EF-P) in bacteria,[5,10,13,14] or by the EF-P homologue, initiation factor eIF5A, in eukaryotes.[18] EF-P and eIF5A are both modified post-translationally, and the respective modifications are critical for the rescue activity of these factors.[5,10,13,18] In *Escherichia coli* and most other γ-proteobacteria, EF-P is hydroxylysyl-β-lysylated by action of YjeA (EpmA), YjeK (EpmB), and YfcM (EpmC),[19−22] whereas in *Pseudomonas* and most β-proteobacteria, EF-P, is L-rhamnosylated by the action of EarP.[22,23] In contrast, archaeal and eukaryotic a/eIF5A is hypusinylated by deoxyhypusine synthase (DHS) and deoxyhypusine hydroxylase (DOHH) (reviewed in refs 22,24). On the basis of the structure of an unmodified EF-P in complex with the ribosome,[25] a model for the post-translational modification of EF-P was constructed, suggesting that it extends toward the peptidyl transferase center

Received: July 16, 2015
Published: September 18, 2015

DOI: 10.1021/jacs.5b07427
J. Am. Chem. Soc. 2015, 137, 12997−13006

of the ribosome. However, given the length of the EF-P and eIF5A modifications, they appear likely to increase the rate of peptide bond formation by contributing to the positioning and stabilization of the peptidyl-Pro-tRNA on the ribosome rather than being directly involved in catalysis.[23,25]

Despite these recent advances in our understanding of polyproline-mediated ribosome stalling and rescue by EF-P, it still remains unclear as to how consecutive proline residues interfere with peptide bond formation to induce translational arrest. Pro is unique among the 20 proteinogenic amino acids by having a pyrrolidine ring spanning the α-carbon (Cα) and nitrogen of the backbone. The cyclic side chain of Pro restricts the possible conformations of the Pro amino acid itself as well as the conformations of the neighboring amino acids. Furthermore, Pro can adopt distinct *cis* and *trans* states, which alter the torsion angle of the peptide bond between Pro and the preceding residue. With the exception of Pro, peptide bonds between all amino acids adopt the energetically favored *trans* conformation, which allows them to avoid steric clashes with the neighboring residues. While the *cis* and *trans* isomers of Pro are essentially isoenergetic (~0.7 kcal/mol difference),[26] more than 90% of Pro in protein structures adopt the *trans* conformation (reviewed in 24,27). Conversion between *cis* and *trans* conformations requires a 180° rotation around the peptide bond and is rather slow and energetically unfavorable (~20 kcal/mol).[28] The use of proline analogues has provided some initial insights into the properties of the cyclic ring that influence peptide bond formation, for example, the use of proline analogues azetidine and γ-thiaproline appears to enhance peptide bond formation when compared with dehydroproline and proline.[6,8] Interestingly, a chiral bias was observed when monitoring the incorporation of 4-*R*/*S*-hydroxylated and fluorinated proline analogues into proteins in vivo.[29] Also the protein folding rates and stability are affected by *cis*/*trans* isomerization and the puckering of the Pro ring.[30] However, further studies in vitro using more extensive sets of proline analogues in the context of polyproline stretches and in the presence and absence of EF-P are necessary to fully understand which properties of Pro contribute to polyproline-mediated translational stalling.

Here we have utilized 12 different proline analogues to investigate why peptide bond formation with proline is slow and how EF-P can catalyze the reaction. We investigate the effects of the Pro ring structure and dynamics and of the analogues' electronic properties on the rate of peptidyl transfer reaction measured by rapid kinetic methods in three different kinetic regimes as well as on the overall protein translation. We analyze the reaction on the ribosome with the help of linear free energy relationships and compare it to the hydrolysis and aminolysis reactions in solution. We also determine the contribution of EF-P and identify the favorable entropy change as the main source of catalysis. The data help to explain why the ribosome stalls at consecutive prolines and how EF-P rescues translation.

RESULTS

Proline Analogues. To understand why consecutive prolines cause ribosome stalling and how EF-P alleviates these pauses, we investigated the effect on translation of Pro-analogues (Pro*, P*) with different structural and electronic properties (Scheme 1a). The importance of the five-membered Pro ring size was evaluated using azetidine-2-carboxylic (Aze) and pipecolic acid (Pip), which have four- and six-membered

Scheme 1. Structures of Pro Derivatives and Experimental Approach

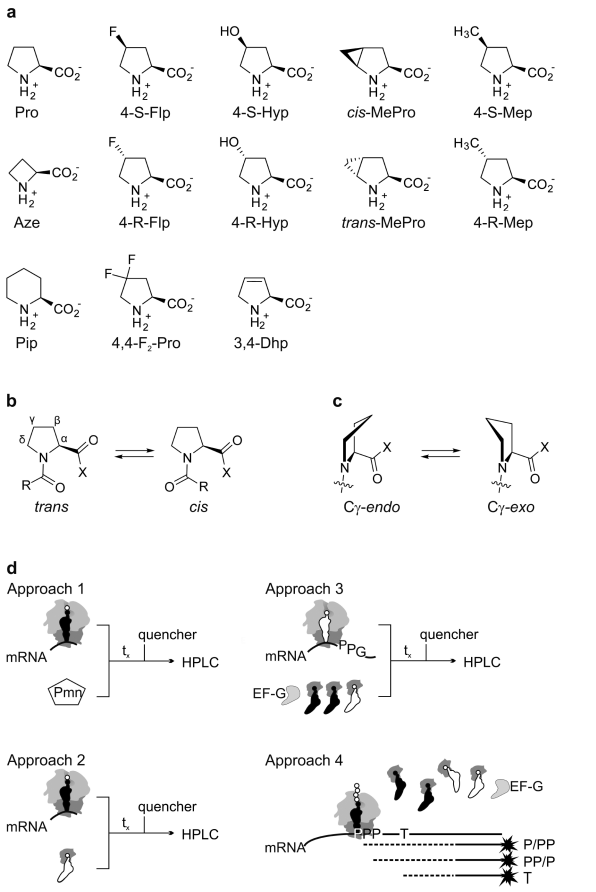

(a) Pro and its derivatives used in the present work. (b) Cis and trans isomers of proline. (c) Cγ exo and Cγ endo puckers of proline. (d) Experimental approaches; $tRNA^{Pro}$ indicated in black. Approach 1, fMetPro*-$tRNA^{Pro}$ reaction with Pmn. Approach 2, fMetPro*-$tRNA^{Pro}$ reaction with Gly-$tRNA^{Gly}$–EF-Tu–GTP. In approaches 1 and 2, post-translocation complexes containing fMetPro*-$tRNA^{Pro}$ in the P site were rapidly mixed with Pmn or Gly-$tRNA^{Gly}$–EF-Tu–GTP. Approach 3, synthesis of the MP*P*G peptide. Initiation complexes (IC) with fMet-$tRNA^{fMet}$ in the P site were mixed with Pro*-$tRNA^{Pro}$ and Gly-$tRNA^{Gly}$ in the presence of EF-Tu, EF-G, and GTP. In approaches 1–3, the reaction was carried out in a quench-flow apparatus. After desired incubation times, the reactions were stopped by the addition of KOH and analyzed by HPLC. Approach 4, the toeprinting assay was employed to monitor the position of ribosomes on an mRNA containing a single PPP motif. The reactions were performed with different Pro analogues in the presence and absence of EF-P and contained all amino acids except for Thr. Because there is only a single Thr codon in the mRNA, located downstream of the PPP motif, ribosomes that translate through the PPP motif become trapped on the Thr codon. Reverse transcription from the 3′ end of the mRNA using a fluorescent primer enables the location of the ribosomes to be determined by the size of the toeprint band following polyacrylamide gel electrophoresis.

rings, respectively. Except for the structure and size differences, the ring variations strongly affect the rate of *cis*–*trans* isomerization (Scheme 1b), with the rates in the range of 10^{-4}–10^{-3} s^{-1} for Pro and 0.1–1 s^{-1} for Aze and Pip.[31] Furthermore, the five-membered Pro ring can adopt one of the two specific puckering conformations which interconvert over the barrier of 2.5 kcal/mol (Scheme 1c).[32] The effect of the conformation of the Pro ring was probed using 3,4-

DOI: 10.1021/jacs.5b07427
J. Am. Chem. Soc. 2015, 137, 12997–13006

dehydroproline (3,4-Dhp) and *cis*-/*trans*-methanoprolines (*cis*/*trans*-MePro), which either arrests the Pro ring in a flat conformation (3,4-Dhp)[33,34] or simulates a particular pucker arrangement (MePro analogues).[35] Finally, the role of the *cis*/*trans* isomers and pucker conformation was tested using C_γ substituted Pro analogues 4-(*R*/*S*)-fluoroproline (4-(*R*/*S*)-Flp), 4-(*R*/*S*)-hydroxyproline (4-(*R*/*S*)-Hyp), and 4-(*R*/*S*)-methylproline (4-(*R*/*S*)-Mep), which differ from Pro in their conformational preferences toward *trans*/*cis* conformers and *exo*/*endo* puckers[36−38] (Supporting Information (SI) Table S1); the two parameters are interdependent.[39] The varying electronegativity of the substituents changes the electron density distribution of the Pro, which is reflected in the pK_a values of their carboxyl and amino groups as measured using model peptides (SI Table S2). While the pK_a values of the amino group are identical within each analogue *R*/*S* pair (except for Hyp), the carboxy pK_a values additionally depend on the orientation of the substituents (SI Table S2). Because of the low isomerization rate, the pK_a values for the *cis* and *trans* isomer can be determined separately.[40,41] The correlation of stereoelectronic characteristics with the modulated activity in the peptidyl transfer reaction may thus allow critical properties to be identified that are responsible for the poor reactivity of Pro in peptide bond formation, and thus may shed light on how EF-P contributes to catalysis of polyproline synthesis.

Experimental Approaches. $tRNA^{Pro}$ was charged with Pro or Pro* using the prolyl-tRNA synthetase. The extent of aminoacylation and the ability of Pro*-$tRNA^{Pro}$ to form the ternary complex (TC) with EF-Tu and GTP was tested by size-exclusion chromatography (SEC) that separates the ternary complex EF-Tu−GTP−Pro*-$tRNA^{Pro}$ from Pro*-$tRNA^{Pro}$ or uncharged tRNA (SI Figure S1). To study the kinetics of proline incorporation into peptides, we used several complementary approaches (Scheme 1d). First, we studied peptide bond formation in a model reaction between the P site-bound fMet-Pro*-$tRNA^{Pro}$ and a mimic of the amino-acyl-tRNA, puromycin (Pmn; 3′-deoxy-*N*,*N*-dimethyl-3′-[(*O*-methyl-L-tyrosyl)amino]adenosine) (approach 1). This reaction was chosen because it yields the rate of the chemistry step rather than of the preceding steps A-site binding, accommodation, or conformational changes.[42,43] Second, to account for the additional effects of the native A-site substrate, we also investigated the effects of Pro* on the reaction between fMet-Pro*-$tRNA^{Pro}$ with Gly-$tRNA^{Gly}$ (in the complex with EF-Tu and GTP) (approach 2) and on the synthesis of a tetrapeptide fMetPro*Pro*Gly when both Pro*- and Gly-ternary complexes are added together in the presence of EF-G (approach 3). Gly-$tRNA^{Gly}$ was chosen due to its low reactivity,[4] which allows us to study peptide bond formation without interference of the decoding steps, in contrast to other aminoacyl-tRNAs, for which the rate of peptide bond formation is limited by the accommodation in the A site.[4,44,45] In approaches 1−3, the reaction was initiated by rapidly mixing the respective ribosome complex with Pmn or the ternary complexes in the quench flow apparatus; the reaction was allowed to proceed for a desired time and stopped by addition of a quencher. The reaction products were analyzed by high performance liquid chromatography (HPLC). Finally, to test whether the observed rate effects can explain Pro-induced ribosome stalling upon translation of entire proteins, we used the toeprinting assay to monitor the position of ribosomes on a model mRNA containing a PPP sequence in the presence of different proline analogues (approach 4). Translation reactions were performed in the absence of the amino acid threonine so that ribosomes that were able to translate through the PPP motif were then caught at a downstream threonine codon, thus enabling the relative levels of stalling and readthrough to be quantitated.

The Ring Size. With Pro, the rate of the Pmn reaction (approach 1) was slow, 0.14 s^{-1} and the time course followed a single-exponential kinetic behavior (Figure 1). The reaction

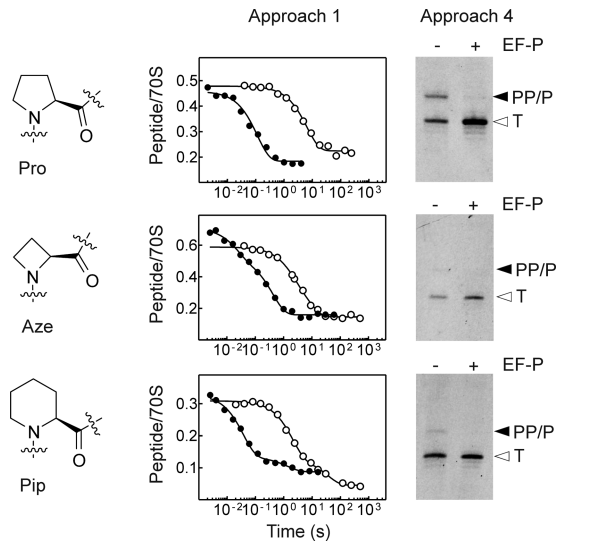

Figure 1. Variations of the amino acid ring size. Approach 1, effect on the kinetics of the fMP*-$tRNA^{Pro}$ reaction with Pmn. Consumption of fMP*-$tRNA^{Pro}$ upon tripeptide formation (fMP*-Pmn) in the absence (open circles) and presence of EF-P (closed circles). P* corresponds to the amino acid listed at the left panel. Approach 4, effect on translation. Stalling at the PPP motif as defined by toeprinting, in the presence and absence of EF-P. Bands at P/PP or PP/P indicate stalling after incorporation of one or two Pro-derivatives, respectively, into the nascent polypeptide chain. T corresponds to stalling site due to a hungry codon downstream of the PPP motif and detects ribosomes that translated through the PPP motif.

with the smaller Aze and larger Pip were both biphasic, with a faster and slower component, suggesting that the complexes formed with Aze and Pip were heterogeneous; the reasons for the heterogeneity are not known. For Aze, the rates of the fast (40%) and slow (60%) reactions differed by a factor of 4; the weighted average corresponding to the overall half-time of the reaction was 0.3 s^{-1}, only 2-fold faster than that with Pro, consistent with the previous data.[6] For Pip, the faster step, 0.5 s^{-1}, was predominant (about 70%) (SI Table S3); the weighted average rate was 0.35 s^{-1}, also about 2-fold faster than with Pro. EF-P accelerated the reaction to an almost identical extent for Pro, Aze, and Pip, namely, about 60-fold in each case. In the translation assay (approach 4) in the absence of EF-P, a portion of ribosomes (38%) stopped after incorporating two Pro residues (PP/P), whereas 62% translated through the polyproline stretch and were then stalled at the Thr (T) codon (Figure 1). Addition of EF-P alleviated stalling, enabling all ribosomes to translate through the poly-Pro stretch to the Thr codon. With Aze and Pip the extent of stalling in the absence of EF-P was reduced (7−17%) compared to Pro, in line with a 2-fold higher rate of peptide bond formation (approach 1). However, the overall tendency, stalling at the PP/P sequence in the absence of EF-P and the rescue in the presence of the factor, was similar for Pro, Aze, and Pip, leading us to conclude that

DOI: 10.1021/jacs.5b07427
J. Am. Chem. Soc. 2015, 137, 12997−13006

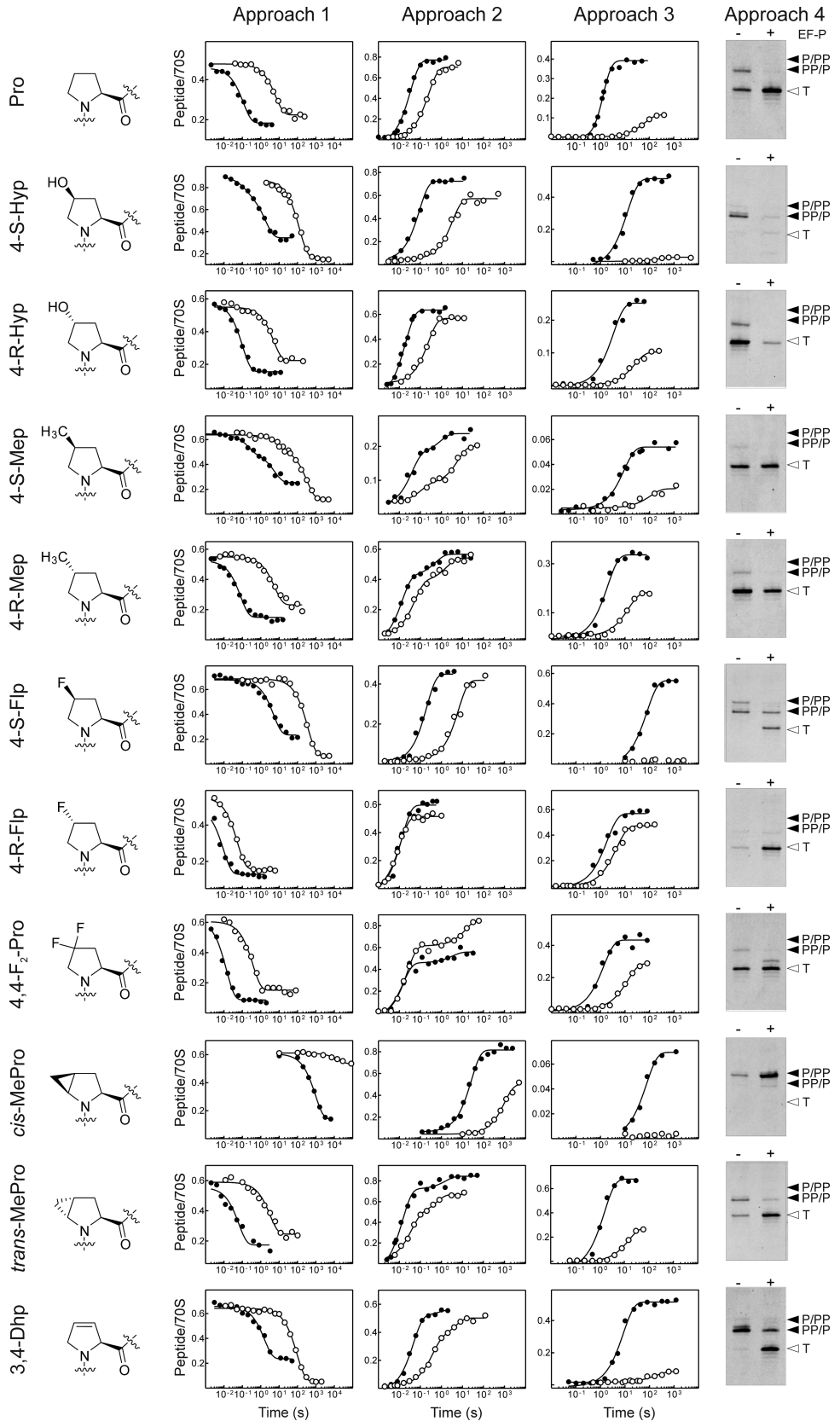

Figure 2. Effects of substituents at the Pro ring. Approach 1, Pmn reaction with Pro analogues. Time courses of fMP*-tRNA^{Pro} decay in the Pmn reaction in the absence (open circles) and presence of EF-P (closed circles). Approach 2, reaction between fMP*-tRNA^{Pro} and Gly-tRNA^{Gly}. Shown are time courses of the fMP*G product formation ± EF-P. Approach 3, synthesis of fMP*P*G. Approach 4, effect on translation. Stalling at the PPP motif as defined by toeprinting, in the presence and absence of EF-P. Bands at P/PP or PP/P indicate stalling after incorporation of one or two Pro-derivatives, respectively, into the nascent polypeptide chain. T corresponds to stalling site due to a Thr downstream of the PPP motif and detects ribosomes that translated through the PPP motif.

DOI: 10.1021/jacs.5b07427
J. Am. Chem. Soc. 2015, 137, 12997−13006

the ring size and the *cis*/*trans* isomerization rate have only a minor effect on Pro-mediated stalling.

Given the small effects and the consistency in the results of approach 1 and 4, alternative types of assays (approaches 2 and 3) were not employed to further analyze Aze and Pip.

Effect of Substituents at the Pro Ring. All Pro analogues with a five-membered Pro ring but with various substitutions (4-(*R*/*S*)-Hyp, 4-(*R*/*S*)-Mep, 4-(*R*/*S*)-Flp, 4,4-F_2-Pro, *cis*/*trans*-MePro, 3,4-Dhp,) can be incorporated into peptides with or without EF-P. In the absence of EF-P, the reaction rates differed by 7 orders of magnitude depending on the analogue, with some being faster or slower than the reaction with proline (Figure 2, SI Table S3). Apart from 4-S-Mep, time courses of the Pmn reaction with all Pro* (approach 1) were single-exponential, with reaction rates between 6×10^{-5} s^{-1} and 21 s^{-1}, compared to 0.14 s^{-1} for Pro, in the absence of EF-P. With 4-*S*-Mep, the reaction was biphasic, dominated (80%) by the slower step (0.003 s^{-1}; SI Table S3). EF-P accelerates k_{pep} for all Pro analogues by a factor between 3 and 100. Consistently with the results obtained with Pmn (approach 1), the rates of tripeptide formation with Gly-tRNA^{Gly} as A-site substrate (approach 2) show the same trend but fall into a slightly narrower kinetic range between Pro analogues compared to the Pmn assay (4 orders of magnitude; Figure 2 and SI Table S3). This can be explained by the existence of the accommodation step for Gly-tRNA^{Gly}, which is rapid compared to the chemistry step for Pro and slow Pro analogues but becomes rate-limiting for highly reactive Pro derivatives. Also here, EF-P accelerates the reaction, except for those analogues that show the high rates (>70 s^{-1}) of peptide bond formation even in the absence of EF-P.

When translation of the tetrapeptide fMPPG was studied (approach 3), little final product was formed with those Pro derivatives (*cis*-MePro, 4-*S*-Flp, and 4-*S*-Hyp) that were poor P-site substrates in the Pmn assay or in reaction with Gly-tRNA^{Gly}. This can be explained by the drop-off of short peptidyl-tRNAs from the stalled ribosome.[5] Thus, in these experiments the reactivity of Pro analogues was not only reflected by their reaction rates but also by the product yield. For all Pro analogues, the amount of final product and the observed rate were consistent with their reactivity observed by approaches 1 and 2. Addition of EF-P accelerated the reaction, prevented drop-off, and thereby increased the level of final product for all Pro analogues, although for *cis*-MePro and 4-*S*-Mep the amount of final product remained very low. The stalling potential of Pro* determined in the translation system (approach 4) was also in good agreement with the observed reactivity in the kinetic assays. Translational stalling with 4-*R*-Hyp, 4-*R*/*S*-Mep, 4,4-F_2-Pro, and 4-*R*-Flp was slightly reduced (8−20%) compared to that with Pro (38%) but also occurred after the second Pro codon (PP/P) and, similar to Pro, was efficiently rescued by EF-P. In contrast, *cis*-MePro, 4-*S*-Hyp, and to a lesser extent, 4-*S*-Flp and 3,4-Dhp, caused translation stalling already after the first Pro codon (P/PP), with no apparent readthrough to the downstream threonine codon. Apart from *cis*-MePro, which leads to exceptionally slow peptide bond formation, EF-P alleviated stalling with all other Pro analogues, suggesting that EF-P can act on a broad range of stalled Pro-like substrates and its function is not restricted by certain chemical/sterical features of proline.

The Intrinsic Reactivity of fMetPro*-tRNA^{Pro}. The variations in the Pro* reactivity on the ribosome could be explained in several different ways. First, the differences in the reaction rates could reflect the intrinsic reactivity differences of the peptidyl-Pro*-tRNAs. Such intrinsic differences should affect any reaction involving the corresponding ester bond, including the hydrolysis or aminolysis reactions in solution, because the nucleophilic attack on carbonyl esters is known to be sensitive toward steric and electronic effects introduced by substitutions in the nonleaving acyl group.[46] Alternatively, the peptidyl transferase center of the ribosome could interfere with the reaction depending on the position and chemical nature of the substitution; such effects are expected to arise on the ribosome but not in solution. As a combination of both scenarios, ribosome-specific effects such as conformational restrictions of the peptidyl chain in the active site could modulate the intrinsic reactivity differences. To dissect the contribution of intrinsic or ribosome-specific effects, we determined the rates of fMetPro*-tRNA^{Pro} hydrolysis and aminolysis in solution. We first measured the rates of hydrolysis reaction as a simple, reliable type of measurement (SI Table S3; Materials and Methods). Because peptide bond formation on the ribosome involves an amine as a nucleophile, we also measured aminolysis of fMetPro*-tRNA^{Pro} in solution using glycinamide as an amine that optimally reflects the nucleophilicity of an A-site tRNA.[47] The aminolysis revealed almost identical substituent effects as the hydrolysis, consistent with results obtained in other model systems.[48] The variation in reaction rates between Pro analogues is surprisingly small compared to that on the ribosome, with a maximal difference of ~18-fold (SI Table S3). Comparison of the hydrolysis/aminolysis rates in solution (k) and the rate of peptide bond formation on the ribosome (k_{pep}) in a log−log plot showed a linear correlation (Figure 3), indicating that the effects of the

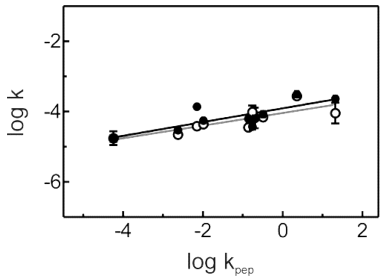

Figure 3. Sensitivity to Pro substitutions in solution and on the ribosome. Correlation between the rate of hydrolysis (k_{hydrol}, closed circles) or aminolysis (k_{aminol}, open circles) of fMP*-tRNA^{Pro} and fMP*-Pmn formation on the ribosome. Average rates from three replicates are plotted, with the symbol size close to SD values.

substituents on the ribosome and in solution reactions follow a similar trend, albeit to a different extent. If the sensitivity of the reaction to Pro* substitutions were the same on and off the ribosome, the slope of the plot were expected to be 1. The slope of ~0.2 suggests that the reaction on the ribosome is much more sensitive toward intrinsic reactivity differences than the reactions in solution.

Activation Parameters. To determine the activation parameters for the reaction with Pro*, we measured the rate/temperature dependence of the Pmn reaction on the ribosome for 4-*S*-Flp and 4-*R*-Flp, the two analogues with the largest difference between the rates for the *S*- and *R*-configurations. These substrates enable activation parameters to be compared because they differ only in the orientation of the same substituent. The Arrhenius plots were linear, with or without

DOI: 10.1021/jacs.5b07427
J. Am. Chem. Soc. 2015, 137, 12997−13006

EF-P (Figure S2). As expected, free energy of activation is smaller for *R*-Flp than for *S*-Flp (Table 1). While activation enthalpy was similar for the two substrates, in the presence or absence of EF-P, the observed rate differences were due to large activation entropy changes, indicating that the reactivity differences between the *R*- and *S*-conformer have an entropic origin and that the catalysis by EF-P is predominantly entropic.

Table 1. Activation Parameters of the Pmn Reaction with fMet-*R*/*S*-Flp-tRNA^{Pro}

Pro*, EF-P	$\Delta G^{\ddagger}$, kcal/mol	$\Delta H^{\ddagger}$, kcal/mol	$T\Delta S^{\ddagger}$, kcal/mol
4-*R*-Flp, no EF-P	16 ± 1	22 ± 2	6 ± 0.6
4-*R*-Flp, EF-P	15 ± 1	24 ± 1	8.4 ± 0.7
4-*S*-Flp, no EF-P	22 ± 1	20 ± 2	−2.2 ± 0.2
4-*S*-Flp, EF-P	19 ± 1	24 ± 1	4.4 ± 0.3

Calculated for 25 °C, $\Delta G^{\ddagger} = RT \ln((k_{pep}\cdot h)/(k_B T))$, $\Delta H^{\ddagger} = E_a - RT$, $T\Delta S^{\ddagger} = \Delta H^{\ddagger} - \Delta G^{\ddagger}$.

DISCUSSION

Reaction in the Absence of EF-P. To quantify the electronic effects of the substituents, we correlated the rates of peptidyl transfer on the ribosome with the electrophilicity of the carbonyl carbon, as represented by the pK_a values of the carboxyl group in model peptides (SI Table S2). The measured reaction rates, e.g., the Pmn reaction, represent a cumulative value for an ensemble of molecules, with their characteristic *cis*−*trans* ratio and the respective elemental pK_a values. To have a pK_a value that is representative of the ensemble, we calculated an impirical pK_a, taking into account the elemental pK_a values for the *cis* and *trans* conformations and the respective ratio for each Pro* (SI Tables S1, S2). The resulting ensemble pK_a values of the proline analogues varied only marginally (2.8−3.6) and did not account for the large rate differences in peptide bond formation on the ribosome (Figure 4). Furthermore, other amino acids such as valine, phenylalanine, and alanine show similar pK_a values (SI Table S2), but the rates of peptide bond formation with the respective peptidyl-tRNAs in the P site are about 100-fold faster than with fMetPro-tRNA[2] (Figure 4). Overall, this indicates that neither the poor Pro reactivity as a P-site substrate nor its stalling properties on the ribosome can be attributed simply to its electrophilicity.

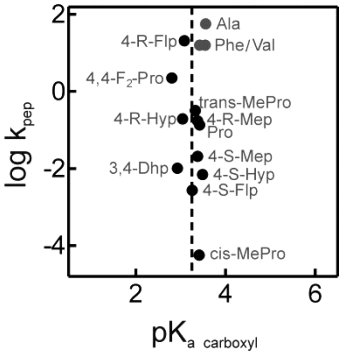

Figure 4. The rate of peptide bond formation on the ribosome vs the electrophilicity of the Pro derivative. Rates are given as average and SD (smaller than the symbol size) obtained from up to four replicates. The p$K_{a\ carboxyl}$ values representative for the mixture of *cis* and *trans* isomers for each given Pro* were calculated as a weighted average taking the *cis*−*trans* equilibrium into account. Rate of fMet-X-Pmn formation, with X = Ala, Phe, Val, was taken from ref 2.

The characteristic features of the Pro five-membered ring are its restricted conformational space, rapidly interconverting *exo* and *endo* pucker conformations and the propensity to form *cis* isomers. When the rates of peptide bond formation of four *R*/*S*-analogue pairs are compared, the *R*-isomers are generally faster (Figure 5a). While *R*- and *S*-configurations pertain to the analogues only and do not explain the slow Pro reaction, the *R*-isomers of 4-Flp and 4-Hyp, as well as *cis*- and *trans*-MePro, favor the *trans* conformation (SI Table S1), which could be relevant for the Pro mechanism. However, direct comparison of the rate of peptide bond formation with the preference for the *trans* conformation does not show any obvious correlation (Figure 5b). Although the type of pucker is not strictly coupled to *cis* or *trans* configuration, *trans*-stereoisomers tend to favor *exo* pucker conformation.[49−51] One exception is *cis*-MePro, which mimics the *endo* pucker conformation but has a high content of *trans*-X-P* bonds (Figure 5c). *Cis*-MePro is exceptionally slow, which suggests that the pucker conformation rather than the *cis*−*trans* preference may determine the rate of peptide bond formation. Furthermore, the orientation of the substituent could cause the observed reactivity differences. Because of its electron donating methyl group, 4-*R*-Mep has a higher content of *cis*-X-P* bonds and prefers the *endo* pucker compared to 4-*S*-Mep. Reactions with 4-*R*-Mep are faster than with 4-*S*-Mep, supporting the conclusion that *R*-analogues are better substrates for the peptidyl transfer reaction than their *S*-counterparts, irrespective of the pucker conformation.

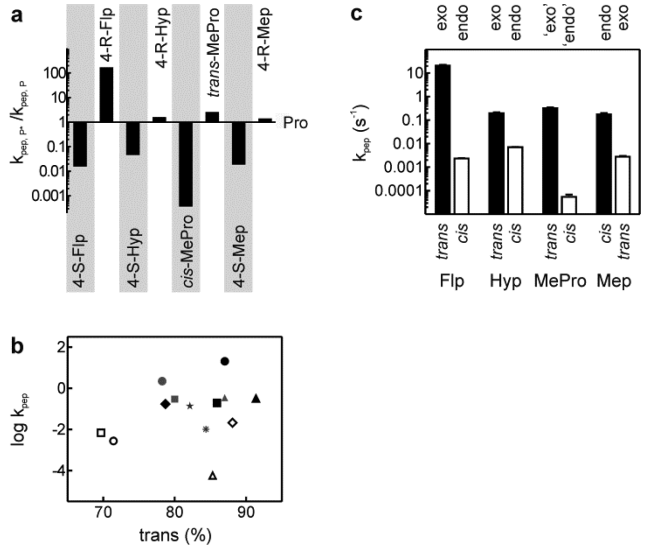

Figure 5. Peptide bond formation is faster with *R* analogues. (a) Relative rates of fMP*-Pmn formation for Pro* normalized to Pro. (b) Influence of trans content of Pro derivatives on rate of fMP*-Pmn formation. 4-(*R*/*S*)-Hyp (squares), 4-(*R*/*S*)-Flp (circles), 4-(*R*/*S*)-Mep (diamonds), *cis*/*trans*-MePro (triangles). *S* isomers (open symbols), *R* isomers (closed symbols). Pro, 3,4-Dhp, 4,4-F2-Pro, Aze, and Pip in gray asterisk, star, circle, triangle, and square, respectively. (c) Effect of the stereochemistry of Pro* on k_{pep} of the reaction with Pmn. Plotted are the k_{pep} values for each pair of analogues that differ only in their substituent orientation at the Cγ atom in the *R*- (black bars) or *S*- (white bars) configuration. Isomer and pucker preference as indicated. Cis and trans MePro are covalently arrested pucker mimics. The average values and SD are calculated from up to four replicates.

DOI: 10.1021/jacs.5b07427
J. Am. Chem. Soc. 2015, 137, 12997−13006

The intrinsic reactivities of aminoacyl-tRNAs with Pro-, Pro* analogues (SI Table S3) or other amino acids[52] in solution are similar. The small reactivity differences between Pro analogues in solution are dramatically increased on the ribosome. While there is no simple explanation for the rate variations between Pro analogues in terms of electrophilicity or preference to a single conformation, the entropic character of substituent effects suggests that the positioning of Pro-tRNA in the peptidyl transferase center of the ribosome is the major determinant for the slow reaction. In this view, the unfavorable positioning on the ribosome exaggerates the differences in the intrinsic reactivity, e.g., by altering the trajectory for the nucleophilic attack.

Catalysis by EF-P. EF-P accelerates peptide bond formation with Pro to a rate which is compatible with the overall translation rate. EF-P increases the reaction rates with all Pro analogues, although the extent of acceleration is more pronounced for the particularly slow substrates (SI Table S3). Calculation of the free energy from the rate acceleration (Figure 6) reveals that EF-P has an averaged catalytic

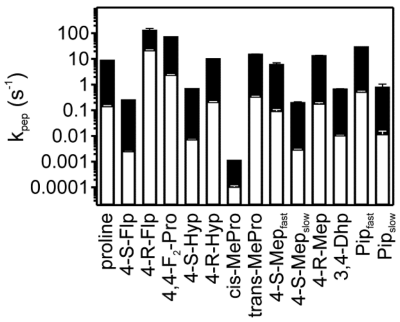

Figure 6. Uniform contribution of EF-P to catalysis. Rates of fMP*-Pmn formation without (white bars) and with EF-P (black bars). Bars represent average rates and SD from up to four replicates.

contribution of −2.5 ± 0.2 kcal/mol for most Pro analogues, except for *cis*-MePro and 4-*R*-Flp. The EF-P effect for *cis*-MePro and 4-*R*-Flp is likely to be somewhat underestimated because for *cis*-MePro the rate of the reaction without EF-P is too slow and for 4-R-Flp the rate in the presence of EF-P is too fast to be determined with high precision.

Comparison of the activation parameters of the reaction with and without EF-P suggests that the acceleration is due to a favorable entropic effect, whereas the enthalpy change is unfavorable, if at all (Table 1 and SI Table S4). The absence of an enthalpic contribution to catalysis argues against an idea that EF-P might contribute to catalysis by donating functionally active groups, which would predict favorable enthalpic effects.[53] This is in line with the observations that EF-P does not reach into the peptidyl transferase center of the ribosome.[25] EF-P and its eukaryotic homologue eIF5A are post-translationally modified at a position that may protrude toward the active site of the ribosome.[19,20,54,55] However, the nature of the modification varies between eukaryotes and different phylogenetic groups of bacteria. Some of these modifications are too short to reach the P-site Pro,[23] indicating a lack of an evolutionary conservation toward a modification that can extend toward the active site. Most likely, the post-translational modifications have evolved to serve another purpose, e.g., stabilization of the CCA end of the P-site tRNA.[5,23] The entropic character of catalysis by EF-P is consistent with the notion that the factor induces a more favorable positioning of the P-site substrate in the peptidyl transferase center. EF-P may also act by contacting the body of the tRNA (ref 25), as suggested by the finding that in some cases even the unmodified EF-P can accelerate Pro incorporation, albeit to a much smaller extent than a fully modified factor.[5] In addition to the positioning effects, favorable entropic term may be due to an improved electrostatic environment at the peptidyl transferase center or a better orientation of water molecules involved in catalysis.[56] Previous computational analysis of the energetics of peptide bond formation on the ribosome suggested that all these effects can contribute to the favorable entropic term.[57−59] While analogous calculations are not feasible so far for Pro-tRNA and EF-P due to the lack of the suitable atomic-resolution structures, in the future, our data on Pro substituent effects may provide a benchmark for the validation of such detailed molecular dynamic simulations.

In summary, the present work suggests that the steric, rather than electronic, properties of Pro make it an exceptionally poor P-site substrate. The mechanism of peptide bond formation entails a concerted proton transfer between the reactive groups and the water molecules in the active site, which requires stabilization by the precisely positioned groups of 23S rRNA in the peptidyl transferase center.[1,56] Steric restrictions may disturb the proton transfer and stabilization of the developing charges. Notably, the existence of the context effect, i.e., modulation of the strength of stalling on Pro runs by a preceding or following amino acid,[12,14−17] indicates that the Pro positioning may be improved by steric properties of the peptidyl moiety of the P-site substrate or compensated by a particular aa-tRNA in the A site. EF-P contributes to catalysis in an entropic way, presumably by providing a better orientation of the P-site Pro-ester or organizing additional electrostatic interactions in the vicinity of the transition state.

MATERIALS AND METHODS

Buffers and Reagents. Buffer A: 50 mM Tris-HCl, pH 7.5 at 37 °C, 70 mM NH_4Cl, 30 mM KCl, and 7 mM $MgCl_2$. Buffer B: 50 mM Tris-HCl, pH 7.5 at 37 °C, 70 mM NH_4Cl, 30 mM KCl, 3.5 mM $MgCl_2$, 0.5 mM spermidine, 8 mM putrescine, and 2 mM DTT. Buffer C: 20 mM Hepes-HCl pH 7.5 at 37 °C, 100 mM KCl, and 7 mM $MgCl_2$. Chemicals were from Sigma-Aldrich, Roche Molecular Biochemicals, or Merck. Radioactive compounds were obtained from Hartmann Analytic. Synthesis and full characterization of Pro analogues will be published elsewhere.[60]

Ribosomes and Proteins. Ribosomes from *E. coli* MRE600, initiation factors (IF1, IF2, IF3), EF-Tu, and EF-G were prepared as described.[5,61] The DNA construct coding for Pro-tRNA synthetase (ProRS) was purchased from the Keio collection;[62] the protein was overexpressed in BL21(DE3) and purified by affinity chromatography on a Protino gravity-flow column (Macherey-Nagel) using the oligohistidine tag. Protein was stored in buffer A containing 50% glycerol; protein concentration was determined by absorbance at 280 nm, assuming an extinction coefficient of 54320 cm^{-1} M^{-1}. Native EF-P was prepared from *E. coli* MRE600 as previously described, and the presence of modifications was confirmed by LC-MS/MS.[5]

mRNAs. The following mRNAs were used (coding sequence is underlined): 5′-GGCAAGGAGGUAAAUAAUGCCGGGUAUU-3′ coding for fMet-Pro-Gly (approaches 1 and 2); 5′-GGCAAGGAGGUAAAUAAUGCCGCCGGGUAUU-3′ coding for fMet-Pro-Pro-Gly (approach 3); the terminal Ile codon was not translated. mRNAs were purchased from IBA.

tRNAs. Native tRNAs ($fMet\text{-}tRNA^{fMet}$, $Phe\text{-}tRNA^{Phe}$, $Gly\text{-}tRNA^{Gly}$) were prepared as described.[5,61] Transcript of $tRNA^{Pro}$ was prepared as follows.[63] Two partially complementary DNA oligomers coding for isoacceptor $tRNA^{Pro}$ with the anticodon CGG fused to T7 RNA-

DOI: 10.1021/jacs.5b07427
J. Am. Chem. Soc. 2015, 137, 12997−13006

polymerase promoter were obtained from IBA (F 5′→3′: AGTTGCTGCAGTA ATACGACTCACTATACGGUGAUUGGCGCAGCCUGGUAGCGCACUUCGUUCG; R 5′→3′: TGGTCGGTGATAGAGGATTCGAACCTCCGACCCCTTCGTCCCGAACGAAGTGCGCTACCAGGCTG), extended by PCR and cloned into pUC19 vector using SMA1 restriction site.[64] PCR with primers (F 5′→3′: TAATACGACTCACTATACG and R 5′→3′: TGmGTCGGTGATAGAGGATTC; where m designates a 2′-*O*-methyl group used to prevent nonspecific 3′mRNA extension by T7 RNA polymerase) resulted in the transcription template (∼100 μg/mL) which was incubated in 40 mM Tris-HCl pH 7.5, 15 mM $MgCl_2$, 2 mM spermidine, 10 mM NaCl, 10 mM DTT supplemented with 3 mM NTPs, 5 mM CMP, 0.01 u/μL PPase, 1.6 u/μL T7 RNA polymerase (Fermentas), and 0.6 u/μL RiboLock RNase inhibitor (Fermentas) for 3 h at 37 °C. The transcript was purified on a HiTrapQ HP column (GE Gealthcare) using a 0−1.1 M NaCl gradient in 50 mM Na acetate pH 5, 10 mM $MgCl_2$. Fractions containing tRNA transcript were collected, phenol extracted, and tRNA was precipitated with ethanol. The tRNA pellet was resolved in H_2O, and concentration was determined by aminoacylation with [^{14}C]Pro. To verify the functional activity of tRNA transcript, its performance was compared to that of native $tRNA^{Pro}$ in all assays used. We found that all kinetics were virtually identical for the native $tRNA^{Pro}$ and $tRNA^{Pro}$ transcript, indicating that the lack of modifications did not interfere with its function in translation or with the EF-P effect (SI Figure S1a). Aminoacylation of $tRNA^{Pro}$ with Pro* was carried out in buffer containing 30 mM Hepes-HCl pH 7.5, 30 mM KCl, 10 mM $MgCl_2$, 1 mM DTT, and 3 mM ATP. $tRNA^{Pro}$ (25 μM) was mixed with Pro or Pro* (2−5 mM) in the presence of ProRS (1 μM) and IPPase (0.5%) and incubated for 30 min at 37 °C. Pro-Rs charged $tRNA^{Pro}$ with any of the Pro* used, albeit with different efficiency. Recognition of Pro*-$tRNA^{Pro}$ by EF-Tu was confirmed by size exclusion chromatography (SEC). Ternary complexes (TC) Pro*-$tRNA^{Pro}$−EF-Tu−GTP were stable for the duration of the following experiments (SI Figure S1c). To study hydrolysis and aminolysis reactions in solution, fMP*-$tRNA^{Pro}$ was extracted from post-translocation complexes (PTC, see next section) with 50 mM NaOAc pH 5, 500 mM KCl, and 100 mM EDTA for 10 min at 37 °C. fMP*-$tRNA^{Pro}$ was purified from the ribosomal components by ultracentrifugation at 260000*g* for 1 h at 4 °C. fMP*-$tRNA^{Pro}$ from the supernatant was further purified as described for tRNA transcript. Additional purification and concentration was obtained by using Centrifugal filter units (Merck) according to the manufacturers' protocol.

Ribosome Complexes. Initiation complexes (IC) were prepared by incubating 70S ribosomes (1 μM) with initiation factors (IF1, IF2, IF3) (1.5 μM each), mRNA (3 μM), GTP (1 mM), and of ^{3}H- or ^{14}C-labeled fMet-$tRNA^{fMet}$ (1.5 μM) in buffer A for 30 min at 37 °C [2]. Purification of complexes was carried out by ultracentrifugation through 400 μL sucrose cushion (1.1 M in buffer A) at 260000*g* for 2 h. Complexes were dissolved in buffer A and stored at −80 °C. If not stated otherwise, ternary complexes were obtained by incubation of EF-Tu (50 μM) with GTP (1 mM), pyruvate kinase (0.1 μg/μL), and phosphoenolpyruvate (3 mM) in buffer A or B for 15 min at 37 °C, followed by addition of Pro*-$tRNA^{Pro}$ (25 μM) or a mixture of Pro*-$tRNA^{Pro}$ and Gly-$tRNA^{Gly}$ and further incubation for 2 min. When Pro*-$tRNA^{Pro}$ was used as A-site substrate, Pro*-$tRNA^{Pro}$−EF-Tu−GTP complex was purified by SEC on a tandem Superdex 75−10/300 GL columns (GE Healthcare)[61,65] and the concentration of the ternary complex was determined photometrically at 260 nm. PTCs were formed by mixing initiation complexes with a 2-fold excess of ternary complexes (Pro*-$tRNA^{Pro}$−EF-Tu−GTP) in buffer A with 14 mM $MgCl_2$. After 5 min incubation at 37 °C EF-G was added (1/10 molar ratio to ribosomes). After 30 s of translocation, ribosome complexes were loaded on a sucrose cushion as described for initiation complexes. To determine the efficiency of complex formation with Pro*-$tRNA^{Pro}$ and thereby the PTC concentration, incorporation of the next amino acid encoded by the mRNA ([^{14}C]Phe or [^{3}H]Gly) was monitored. For most analogues the efficiency of PTC formation was between 70 and 90%. The efficiency of PTC formation with 4-*S*-Mep-, 4-*R*-Mep-, Aze-, and Pip-$tRNA^{Pro}$ reached 20−50%.

Toeprinting Assay. The toeprinting assays were performed as described previously.[17] Briefly, in vitro translation reactions of the PPPFT* template (TTAATACGACTCACTATAGGGGAATTGTGAGCGGATAACAATTCCCCTCTAGAAATAATTTTGTTTAACTTTAAGAAGGAGATATACATATGCATCATCATCATCATCACAAGAATATACGTAACTTTTCGATCATAGCTCACATTGACCACCTGCCGCCGCCGTTTACCTAATAAGAGCTCGGTAAATCGACGCTGTCTGACCGTATTATCCAGATCTGCGGTGGCCTGTCTGACCGTGAAATGGAGGCGCAGGTTCTC) with ATG start codon, consecutive proline triplet CCGCCGCCG, and ACC Thr codon, were carried out in the PURExpress Δaa ΔtRNA kit (New England Biolabs) with the presence of 2 pmol of the reverse primer (5′-GAGAACCTGCGCCTCCATTTCACGGTC-3′) labeled with 6-FAM at 5′ end (Metabion). Translation was performed in the absence of the amino acid threonine to monitor ribosomes that do not stall at the PPP motif by trapping them on the downstream ACC (Thr) codon and in the presence of either Pro or Pro* at the concentration 0.1 mM. To ensure efficient aminoacylation of $tRNA^{Pro}$, reactions were preincubated without the template for 5 min at 37 °C. Upon addition of template, reactions were incubated for 30 min at 37 °C. Where indicated, EF-P (1 μM) was added. Subsequently, 100 units of reverse transcriptase (RT) Superscript III (Life Technologies) and dNTP mix to the final concentration of 400 μM was added. The RT reaction was then incubated for additional 30 min at 37 °C. Products of the reactions were purified using Nucleotide Removal Kit (Qiagen) and lyophilized. The lyophilized pellets were resuspended in a formamide loading dye solution and applied on the 7% urea-acrylamide gel. Fluorescence of samples was detected using Typhoon FLA 9500 scanner. Intensity of stalled bands was acquired using ImageJ. To correlate the toeprint bands with the site of ribosome stalling, sequencing reactions were performed on the PPPFT* template using coupled transcription-translation (PURExpress kit) without addition of amino acids and tRNA. Reactions were supplemented with 6-FAM-labeled primer used for toeprinting and incubated for 30 min, followed by addition of 100 units of Superscript III (Life Technologies) and ddNTP/dNTP mix (Roche) to the final concentration of 4 mM/400 μM, respectively. Reactions were then further incubated for 30 min at 37 °C, and the products were purified and subjected to electrophoresis as described for the toeprinting reactions.

Kinetics. Time courses were obtained either by manual pipetting or in a quench flow apparatus (KinTek Laboratories, Inc.) by mixing equal volumes of reactants, incubating for the desired time, and stopping the reaction by addition of KOH (0.5 M), followed by hydrolysis of tRNA (for 30 min at 37 °C) and neutralization with glacial acetic acid. If not stated otherwise, substrates and products were separated on reversed phase columns (LiChrospher 100 RP-8 or Chromolith RP8 100−4.6 mm column, Merck) using 0−65% acetonitrile gradient in 0.1% TFA and quantified by double-label scintillation counting.

The Puromycin Reaction was performed by mixing equal volumes of PTC (0.15 μM final) and Pmn (10 mM final) with or without EF-P (3 μM final) in buffer A at 37 °C.[42] For fMet-Pro*-Pmn formation, the decay of fMet-Pro* was monitored and the rate was determined by single- or double-exponential fitting of [educt]/([product] + [educt]) vs time. With 4-*S*-Hyp, the substrate consumption was visualized. For the very rapid reaction with 4-*R*-Flp in the presence of EF-P at 37 °C, the reaction occurred partially within the dead time of the quench flow apparatus (2 ms). To correct for the lack of information at the initial time points, the starting concentration of the P-site substrate was determined prior to the reaction and set constant in one-exponential fitting.

*fMP*G Formation.* PTC(P*) (0.2 μM final) was mixed with TC(G) (10 μM final) with or without EF-P (3 μM final) in buffer B at 37 °C.[5]

*fMP*P*G Formation.* Purified initiation complex (0.2 μM final) primed with mRNA encoding for MPPG was mixed with ternary complexes TC(P*) (purified by SEC) and TC(G) (2 μM final each)

DOI: 10.1021/jacs.5b07427
J. Am. Chem. Soc. 2015, 137, 12997−13006

in the presence of EF-G (1 μM) with or without EF-P (3 μM final) in buffer B at 37 °C. The observed rate comprises all kinetic steps of three elongation cycles which include accommodation of tRNAs, peptide bond formation, and translocation.

Hydrolysis of fMP-tRNA^{Pro}.* f[^{3}H]Met-Pro*-tRNA^{Pro} (0.5 μM) was hydrolyzed in buffer C at 37 °C. Reactions were stopped by addition of 10% TCA with 50% EtOH, and intact peptidyl-tRNA was collected by nitrocellulose filtration and quantified by ^{3}H scintillation counting. In some cases, the population of complexes was heterogeneous due to incomplete A-site occupancy with ribosomes containing either f[^{3}H]MetPro*-tRNA^{Pro} or f[^{3}H]Met-tRNA^{fMet} which could not be distinguished by scintillation counting. The hydrolysis rates for the two species could be assigned based on the two-exponential courses of the reaction, knowing the intrinsic decay rate of f[^{3}H]Met-tRNA^{fMet}. In other cases where the A-site occupancy was high, the contribution of fMet-tRNA^{fMet} was sufficiently small to be neglected.

Aminolysis of Peptidyl-tRNA. Aminolysis was performed in buffer C containing 1 M glycinamide corresponding to 0.2 M unprotonated glycinamide (Sigma-Aldrich) at 37 °C.[47] Concentration of unprotonated glycinamide at pH 7.5 was calculated using the published pK_a of 8.2.[66] In the presence of amine, the rate of peptidyl-tRNA decomposition (k_{decay}) reflects the sum of two competing reactions, aminolysis and hydrolysis. The rate of aminolysis was calculated from the decay rate in the presence of glycinamide and the hydrolysis rate according to the equation $k_{aminol} = k_{decay} - k_{hydrol}$.

Calculation of Activation Energies. The activation parameters were determined on the basis of Arrhenius and Eyring equations for 25 °C. The free energy of activation was calculated with $\Delta G^{\ddagger} = -RT \ln((k \cdot h)/(k_B \cdot T))$, where R is the gas constant, T the absolute temperature, and h and k_B are the Planck's and Boltzmann's constants, respectively. The activation energy (E_a) was determined from the slope of the Arrhenius plot, with $E_a = -\text{slope} \times R$ and the enthalpy of activation according to $\Delta H^{\ddagger} = E_a - RT$. The entropy of activation was obtained from $T\Delta S^{\ddagger} = \Delta H^{\ddagger} - \Delta G^{\ddagger}$.

■ ASSOCIATED CONTENT

Supporting Information

The Supporting Information is available free of charge on the ACS Publications website at DOI: 10.1021/jacs.5b07427.

Characterization of chemical and biochemical compounds, rate constants of peptide bond formation, and thermodynamic parameters (PDF)

■ AUTHOR INFORMATION

Corresponding Authors

*rodnina@mpibpc.mpg.de (M.V.R.)
*wilson@lmb.uni-muenchen.de (D.N.W.)
*nediljko.budisa@tu-berlin.de (N.B.)

Present Address

⊥Agata L. Starosta, Institute for Cell and Molecular Biosciences, Newcastle University, Newcastle upon Tyne, UK.

Author Contributions

#L.K.D. and I.W. contributed equally.

Notes

The authors declare no competing financial interest.

■ ACKNOWLEDGMENTS

We thank Olaf Geintzer, Sandra Kappler, Christina Kothe, Anna Pfeiffer, Theresia Uhlendorf, Tanja Wiles, and Michael Zimmermann for expert technical assistance. The work was supported by Max Planck Society (M.V.R.) and by the grants of the Deutsche Forschungsgemeinschaft (FOR 1805 to M.V.R., I.W., N.B., and D.N.W.), FP7 EU-funded METACODE-Consortium and UniCat Excellence Cluster of TU Berlin (N.B. and V.K.), and Center for Integrated Protein Science Munich (D.N.W.).

■ REFERENCES

(1) Rodnina, M. V. *Curr. Opin. Struct. Biol.* **2013**, *23*, 595.
(2) Wohlgemuth, I.; Brenner, S.; Beringer, M.; Rodnina, M. V. *J. Biol. Chem.* **2008**, *283*, 32229.
(3) Pavlov, M. Y.; Watts, R. E.; Tan, Z.; Cornish, V. W.; Ehrenberg, M.; Forster, A. C. *Proc. Natl. Acad. Sci. U. S. A.* **2009**, *106*, 50.
(4) Johansson, M.; Ieong, K. W.; Trobro, S.; Strazewski, P.; Aqvist, J.; Pavlov, M. Y.; Ehrenberg, M. *Proc. Natl. Acad. Sci. U. S. A.* **2011**, *108*, 79.
(5) Doerfel, L. K.; Wohlgemuth, I.; Kothe, C.; Peske, F.; Urlaub, H.; Rodnina, M. V. *Science* **2013**, *339*, 85.
(6) Muto, H.; Ito, K. *Biochem. Biophys. Res. Commun.* **2008**, *366*, 1043.
(7) Ito, K.; Chiba, S. *Annu. Rev. Biochem.* **2013**, *82*, 171.
(8) Hayes, C. S.; Bose, B.; Sauer, R. T. *J. Biol. Chem.* **2002**, *277*, 33825.
(9) Tanner, D. R.; Cariello, D. A.; Woolstenhulme, C. J.; Broadbent, M. A.; Buskirk, A. R. *J. Biol. Chem.* **2009**, *284*, 34809.
(10) Woolstenhulme, C. J.; Parajuli, S.; Healey, D. W.; Valverde, D. P.; Petersen, E. N.; Starosta, A. L.; Guydosh, N. R.; Johnson, W. E.; Wilson, D. N.; Buskirk, A. R. *Proc. Natl. Acad. Sci. U. S. A.* **2013**, *110*, E878.
(11) Ingolia, N. T.; Lareau, L. F.; Weissman, J. S. *Cell* **2011**, *147*, 789.
(12) Woolstenhulme, C. J.; Guydosh, N. R.; Green, R.; Buskirk, A. R. *Cell Rep.* **2015**, *11*, 13.
(13) Ude, S.; Lassak, J.; Starosta, A. L.; Kraxenberger, T.; Wilson, D. N.; Jung, K. *Science* **2013**, *339*, 82.
(14) Peil, L.; Starosta, A. L.; Lassak, J.; Atkinson, G. C.; Virumae, K.; Spitzer, M.; Tenson, T.; Jung, K.; Remme, J.; Wilson, D. N. *Proc. Natl. Acad. Sci. U. S. A.* **2013**, *110*, 15265.
(15) Hersch, S. J.; Wang, M.; Zou, S. B.; Moon, K. M.; Foster, L. J.; Ibba, M.; Navarre, W. W. *mBio* **2013**, *4*, e00180-13.
(16) Elgamal, S.; Katz, A.; Hersch, S. J.; Newsom, D.; White, P.; Navarre, W. W.; Ibba, M. *PLoS Genet.* **2014**, *10*, e1004553.
(17) Starosta, A. L.; Lassak, J.; Peil, L.; Atkinson, G. C.; Virumae, K.; Tenson, T.; Remme, J.; Jung, K.; Wilson, D. N. *Nucleic Acids Res.* **2014**, *42*, 10711.
(18) Gutierrez, E.; Shin, B. S.; Woolstenhulme, C. J.; Kim, J. R.; Saini, P.; Buskirk, A. R.; Dever, T. E. *Mol. Cell* **2013**, *51*, 35.
(19) Navarre, W. W.; Zou, S. B.; Roy, H.; Xie, J. L.; Savchenko, A.; Singer, A.; Edvokimova, E.; Prost, L. R.; Kumar, R.; Ibba, M.; Fang, F. C. *Mol. Cell* **2010**, *39*, 209.
(20) Yanagisawa, T.; Sumida, T.; Ishii, R.; Takemoto, C.; Yokoyama, S. *Nat. Struct. Mol. Biol.* **2010**, *17*, 1136.
(21) Peil, L.; Starosta, A. L.; Virumae, K.; Atkinson, G. C.; Tenson, T.; Remme, J.; Wilson, D. N. *Nat. Chem. Biol.* **2012**, *8*, 695.
(22) Roy, H.; Zou, S. B.; Bullwinkle, T. J.; Wolfe, B. S.; Gilreath, M. S.; Forsyth, C. J.; Navarre, W. W.; Ibba, M. *Nat. Chem. Biol.* **2011**, *7*, 667.
(23) Lassak, J.; Keilhauer, E.; Furst, M.; Wuichet, K.; Godeke, J.; Starosta, A. L.; Chen, J. M.; Sogaard-Andersen, L.; Rohr, J.; Wilson, D. N.; Haussler, S.; Mann, M.; Jung, K. *Nat. Chem. Biol.* **2015**, *11*, 266.
(24) Dever, T. E.; Gutierrez, E.; Shin, B. S. *Crit. Rev. Biochem. Mol. Biol.* **2014**, *49*, 413.
(25) Blaha, G.; Stanley, R. E.; Steitz, T. A. *Science* **2009**, *325*, 966.
(26) Owens, N. W.; Braun, C.; O'Neil, J. D.; Marat, K.; Schweizer, F. *J. Am. Chem. Soc.* **2007**, *129*, 11670.
(27) Yaron, A.; Naider, F.; Scharpe, S. *Crit. Rev. Biochem. Mol. Biol.* **1993**, *28*, 31.
(28) Fischer, S.; Dunbrack, R. L.; Karplus, M. *J. Am. Chem. Soc.* **1994**, *116*, 11931.
(29) Larregola, M.; Moore, S.; Budisa, N. *Biochem. Biophys. Res. Commun.* **2012**, *421*, 646.
(30) Steiner, T.; Hess, P.; Bae, J. H.; Wiltschi, B.; Moroder, L.; Budisa, N. *PLoS One* **2008**, *3*, e1680.

DOI: 10.1021/jacs.5b07427
J. Am. Chem. Soc. 2015, 137, 12997−13006

(31) Kern, D.; Schutkowski, M.; Drakenberg, T. *J. Am. Chem. Soc.* **1997**, *119*, 8403.
(32) Kang, Y. K.; Choi, H. Y. *Biophys. Chem.* **2004**, *111*, 135.
(33) Kang, Y. K.; Park, H. S. *Biopolymers* **2009**, *92*, 387.
(34) Flores-Ortega, A.; Casanovas, J.; Zanuy, D.; Nussinov, R.; Aleman, C. *J. Phys. Chem. B* **2007**, *111*, 5475.
(35) Hanessian, S.; Reinhold, U.; Gentile, G. *Angew. Chem., Int. Ed. Engl.* **1997**, *36*, 1881.
(36) Panasik, N., Jr.; Eberhardt, E. S.; Edison, A. S.; Powell, D. R.; Raines, R. T. *Int. J. Pept. Protein Res.* **1994**, *44*, 262.
(37) DeRider, M. L.; Wilkens, S. J.; Waddell, M. J.; Bretscher, L. E.; Weinhold, F.; Raines, R. T.; Markley, J. L. *J. Am. Chem. Soc.* **2002**, *124*, 2497.
(38) Bretscher, L. E.; Jenkins, C. L.; Taylor, K. M.; DeRider, M. L.; Raines, R. T. *J. Am. Chem. Soc.* **2001**, *123*, 777.
(39) Shoulders, M. D.; Raines, R. T. *Annu. Rev. Biochem.* **2009**, *78*, 929.
(40) Hunston, R. N.; Gerothanassis, I. P.; Lauterwein, J. *J. Am. Chem. Soc.* **1985**, *107*, 2654.
(41) Bedford, G. R.; Sadler, P. J. *Biochim. Biophys. Acta, Gen. Subj.* **1974**, *343*, 656.
(42) Katunin, V. I.; Muth, G. W.; Strobel, S. A.; Wintermeyer, W.; Rodnina, M. V. *Mol. Cell* **2002**, *10*, 339.
(43) Sievers, A.; Beringer, M.; Rodnina, M. V.; Wolfenden, R. *Proc. Natl. Acad. Sci. U. S. A.* **2004**, *101*, 7897.
(44) Wohlgemuth, I.; Pohl, C.; Rodnina, M. V. *EMBO J.* **2010**, *29*, 3701.
(45) Pape, T.; Wintermeyer, W.; Rodnina, M. V. *EMBO J.* **1998**, *17*, 7490.
(46) Fersht, A. *Structure and Mechanism in Protein Science: A guide to Enzyme Catalysis and Protein Folding*; W. H. Freeman and Company: New York, 1999.
(47) Schroeder, G. K.; Wolfenden, R. *Biochemistry* **2007**, *46*, 4037.
(48) Bruice, T. C.; Hegarty, A. F. *Proc. Natl. Acad. Sci. U. S. A.* **1970**, *65*, 805.
(49) Hinderaker, M. P.; Raines, R. T. *Protein Sci.* **2003**, *12*, 1188.
(50) Milner-White, E. J.; Bell, L. H.; Maccallum, P. H. *J. Mol. Biol.* **1992**, *228*, 725.
(51) Vitagliano, L.; Berisio, R.; Mastrangelo, A.; Mazzarella, L.; Zagari, A. *Protein Sci.* **2001**, *10*, 2627.
(52) Hentzen, D.; Mandel, P.; Garel, J. P. *Biochim. Biophys. Acta, Nucleic Acids Protein Synth.* **1972**, *281*, 228.
(53) Wolfenden, R.; Snider, M.; Ridgway, C.; Miller, B. *J. Am. Chem. Soc.* **1999**, *121*, 7419.
(54) Ambrogelly, A.; O'Donoghue, P.; Soll, D.; Moses, S. *FEBS Lett.* **2010**, *584*, 3055.
(55) Aoki, H.; Xu, J.; Emili, A.; Chosay, J. G.; Golshani, A.; Ganoza, M. C. *FEBS J.* **2008**, *275*, 671.
(56) Polikanov, Y. S.; Steitz, T. A.; Innis, C. A. *Nat. Struct. Mol. Biol.* **2014**, *21*, 787.
(57) Sharma, P. K.; Xiang, Y.; Kato, M.; Warshel, A. *Biochemistry* **2005**, *44*, 11307.
(58) Trobro, S.; Aqvist, J. *Proc. Natl. Acad. Sci. U. S. A.* **2005**, *102*, 12395.
(59) Wallin, G.; Aqvist, J. *Proc. Natl. Acad. Sci. U. S. A.* **2010**, *107*, 1888.
(60) Kubyshkin, V.; Durkin, P.; Budisa, N. Submitted for publication.
(61) Gromadski, K. B.; Rodnina, M. V. *Mol. Cell* **2004**, *13*, 191.
(62) Baba, T.; Ara, T.; Hasegawa, M.; Takai, Y.; Okumura, Y.; Baba, M.; Datsenko, K. A.; Tomita, M.; Wanner, B. L.; Mori, H. *Mol. Syst. Biol.* **2006**, *2*, 2006.0008.
(63) Brown, E. L.; Belagaje, R.; Ryan, M. J.; Khorana, H. G. *Methods Enzymol.* **1979**, *68*, 109.
(64) Himeno, H.; Hasegawa, T.; Ueda, T.; Watanabe, K.; Miura, K.; Shimizu, M. *Nucleic Acids Res.* **1989**, *17*, 7855.
(65) Rodnina, M. V.; Fricke, R.; Kuhn, L.; Wintermeyer, W. *EMBO J.* **1995**, *14*, 2613.
(66) Good, N. E.; Winget, G. D.; Winter, W.; Connolly, T. N.; Izawa, S.; Singh, R. M. *Biochemistry* **1966**, *5*, 467.

DOI: 10.1021/jacs.5b07427
J. Am. Chem. Soc. 2015, 137, 12997−13006